METEOROLOGICAL REPRESENTIVITY ANALYSIS AND MODELING THE ATMOSPHERIC DISPERSION OF A POWER PLANT PLUME

K. PHILIPPOPOULOS, G.KARVOUNIS and D.DELIGIORGI

National and Kapodistrian University of Athens, Department of Physics,
Physics of Atmospheric Environment Lab, Athens, Greece
e-mail: despo@phys.uoa.gr

EXTENDED ABSTRACT

Modeling the turbulent diffusion of atmospheric pollutants in the planetary boundary layer is a complex task and various approximate solutions have been proposed. In this study the Gaussian approach is adopted for the estimation of ground-level sulphur dioxide concentrations in the region of a diesel power generating plant. A detailed spatial and temporal analysis of the input meteorological parameters is performed in order to determine their ability to characterize the transport and dispersion conditions in the area of concern. The examined parameters are wind speed and direction, atmospheric stability and mixing height. For this purpose, a two-year data set (August 2004 – July 2006) is used from six meteorological monitoring stations operational in the region.

A qualitative assessment of the wind field homogeneity is performed by comparing the Kernel density plots for each station. Local flows such as sea and land breezes, upslope and downslope winds affect the observations greatly, leading to a non-homogenous wind field. This is also justified with the similarity quantitative analysis. Atmospheric stability is commonly evoked in many dispersion studies as the basic parameter characterizing the turbulent state of the atmosphere and its dispersion capabilities. In this study, Pasquill-Gifford (P-G) stability classes are estimated using the Turner and the Sigma-A schemes. The two schemes are compared for Souda and Platanias stations and results exhibit their inconsistency, which has serious implications in air quality modeling. The spatial homogeneity of Atmospheric Stability is assessed by calculating joint frequencies of occurrence of each stability class for all possible pairs of stations. Considerable discrepancies are found for every case with the exception being for those under neutral conditions. The hourly frequency distributions of stability classes for each station reveal the effect of topography on Atmospheric Stability for each station. Hourly mixing height values are calculated for each station by using the experimental Nozaki model which uses routinely measured surface meteorological data. Their similarity degree is low as a result of the poor meteorological homogeneity of the region.

In order to achieve accuracy with a Gaussian model, calculations should be carried out within a region where spatial and temporal meteorological homogeneity exists. Souda station is found to represent adequately the dispersion conditions of the proximate area of the power plant. Several factors, including proximity to the modeled source, land-use and cover characteristics, elevation and wind speed and direction, are incorporated in determining the area of confidence for the Gaussian model. The numerical experiments of the case studies indicate that such a model is capable of predicting the general pattern of ground-level concentrations of SO_2 in the proximate area of the power plant.

Keywords: Air Quality, Dispersion Modeling, Atmospheric Stability, Wind, Mixing Height

1. INTRODUCTION

Steady-state Gaussian models are widely used to assess the ambient air quality of a desired region. They require meteorological data from a single meteorological station and assume this data to be applicable for the entire modeling domain. This paper, initially, discusses representivity issues of measured and estimated meteorological parameters which are used as inputs in such models when applied to inhomogeneous terrains. Limitations associated with the use of Gaussian models in complex topography involve a determination of a sub-area with uniform meteorological and dispersion conditions.

The study area is at the southeastern part of the Chania Plain, located on the island of Crete, Greece. The greater area is constricted by physical boundaries. These are the White Mountains on its southern side and the Aegean coastline on its northern and eastern part. A diesel power generating plant (DEH) is situated on the outskirts of the city of Chania with seven stacks of different technical and operational specifications. A meteorological network of six stations namely, Souda (SOU), Platanias (PLA), Malaxa (MAL), the Technical Educational Institute of Crete (TEI), Pyrovoliko (PBK) and the Military Airport of Souda (AER), operate in the greater region of Chania (see Figure 5). These stations cover the main topographical features and land-use characteristics of the region. In this study a two year data set (August 2004 – July 2006) of wind speed and direction, temperature, relative humidity, total cloud cover and ceiling height is used.

2. HOMOGENEITY ASSESSMENT OF METEOROLOGICAL PARAMETERS

Topography, as well as in-homogeneity of thermal and dynamic properties of the surface, causes distortion of atmospheric flow and turbulence. Air flow in dispersion modelling is typically parameterized by measurements of wind, and turbulence by atmospheric stability and mixing height. An extensive meteorological network enables the assessment of the spatial meteorological homogeneity in a region with complex topographical features.

2.1. Wind Speed and Direction Assessment

A qualitative analysis of wind field homogeneity can be performed by plotting each station's observations in the u-v plane, where each wind speed vector is represented by a single point. The local point density can be calculated by using the Kernel Density Estimation [1], which in our case is expressed by the following formula :

$$\hat{f}_h(\vec{x}) = \frac{1}{N h^2} \sum_{i=1}^{N} G\left(\frac{\vec{x} - \vec{x}_i}{h}\right)$$

where G is the two-dimensional Gaussian distribution, h the Kernel band-width and $\mathbf{x}_1,\ldots,\mathbf{x}_N$ the observations. The resulting diagrams, which can be considered as an alternative representation of wind roses, are presented for all stations in Figure 1.

From these plots, the in-homogeneity of the wind field along with the exposure of each station to different local conditions is apparent. By examining the densities of the Souda and Malaxa stations, which are geographically proximate, a two peak distribution is observed. However, it is observed a considerable scatter at the station of Malaxa which is attributed to differences is altitude and terrain. The considerable differences in their prevailing wind directions between the Souda and the TEI stations are due to the proximity of the TEI station to the Aegean coastline and thus, its observations are highly affected by sea and land breeze circulations. Platanias measurements exhibit considerable scatter and are mainly influenced by downslope winds, while the Pyrovoliko station is mainly influenced by upslope winds due to its location (elevated station in the North-Eastern part of the Chania peninsula). Airport station observations are mainly affected by Northwesterly winds as a mountain barrier located to the Northeast blocks the Northeasterly flow.

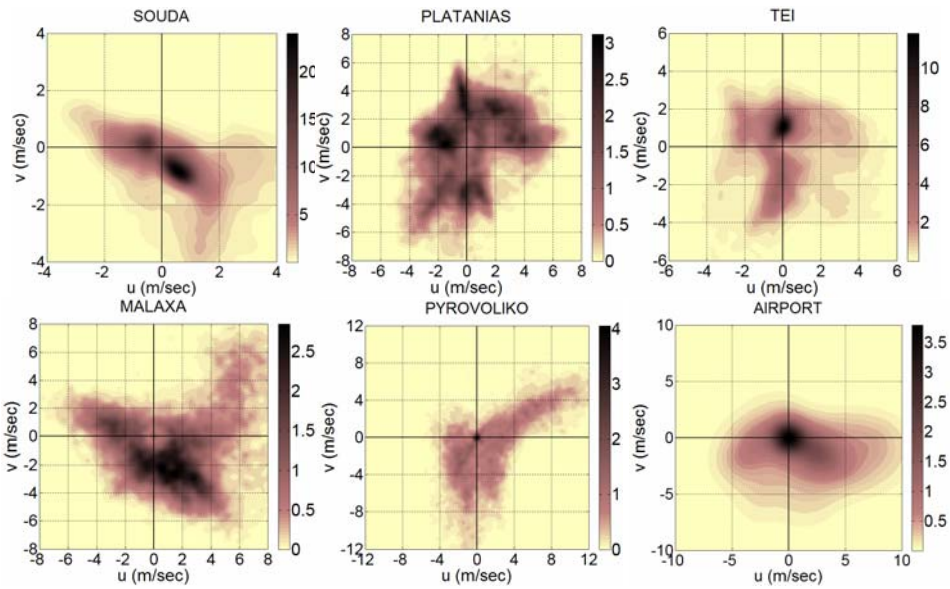

Figure 1: Gaussian Kernel density estimation of wind vectors, using a 0.2 bandwidth. The color-scales correspond to point density, measured in percentage of points per $(m/sec)^2$.

A quantitative similarity test for the wind time series (see Figure 2) is performed by using the similarity curves. They calculate percentages of similar concurrent observations between two time series. The notion of similarity is expressed through parameter R, which is used to define whether two observations are considered to be similar. Their formulation is described in the equation below:

$$s_{ab}(R) = \frac{1}{N}\sum_{i=1}^{N} I_i \quad \text{where} \quad I_i = \begin{cases} 1 & \left\|\vec{v}_{a,i} - \vec{v}_{b,i}\right\| \le R \\ 0 & \text{otherwise} \end{cases}$$

where $\vec{v}_{a,1}, \vec{v}_{a,2}, ..., \vec{v}_{a,N}$ and $\vec{v}_{b,1}, \vec{v}_{b,2}, ..., \vec{v}_{b,N}$ is the first and second time series respectively and $s_{ab}(R)$ represents the percentage of pairs $\left(\vec{v}_{a,i}, \vec{v}_{b,i}\right)$ with a distance less than R.

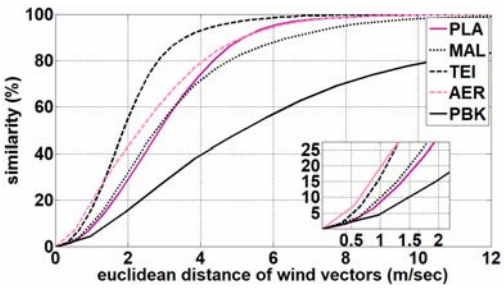

Figure 2: Similarity curves for Souda station.

The above curves indicate a poor agreement between each station and Souda. For a tolerance of less than 1.3 m/sec, Souda station observations are similar to those of the Airport with a percentage of 27%. By selecting higher tolerance values the TEI station exhibits the best overall similarity.

2.2. Atmospheric Stability Assessment

The most common stability classification scheme is the Pasquill-Gifford (P-G), which defines six stability classes namely A (highly unstable), B (moderately unstable), C (slightly unstable), D (neutral), E (moderately stable), and F (extremely stable). Stability class G was added to the initial scheme, to represent low wind night-time stable conditions [2]. Several methodologies exist for the estimation of the P-G stability classes.

In our study, initially, we compared the Turner and Sigma-A schemes for two monitoring stations (see Table 1). The first method uses solar altitude, total cloud cover and ceiling height to calculate the Net Radiation Index (NRI), which in combination with wind speed gives the estimate of the stability classes [3]. The Sigma–A method is a turbulence-based method which uses the standard deviation of the wind direction. Corrections to the initial stability class estimations are applied based on daytime and night-time conditions and mean wind speeds [4].

Table 1: Variance (%) of the Sigma-A results with respect to Turner for Souda and Platanias Stations.

SOU		Sigma-A						PLA		Sigma-A					
		A	B	C	D	E	F			A	B	C	D	E	F
Turner	A	74.6	16.1	8.4	0.9	--	--	Turner	A	34.8	31.4	27.5	6.3	--	--
	B	50.8	23.5	19.8	5.9	--	--		B	27.9	33.8	31.9	6.4	--	--
	C	46.8	16.4	28.4	8.5	--	--		C	18.4	20.9	44.2	16.6	--	--
	D	22.1	15.7	23.6	25.8	2.4	10.4		D	6.0	7.7	19.9	60.5	4.6	1.3
	E	5.4	4.6	4.7	37.0	18.3	30.1		E	1.6	2.4	5.5	61.2	19.1	10.3
	F	6.7	1.6	1.7	16.8	13.2	60.0		F	4.4	2.1	2.5	34.9	21.4	34.7

The overall agreement of the two methodologies is 42.3% for the Souda station and 40.7% for the Platania station. These low percentages, along with the considerable variation of the Sigma-A results, with respect to Turner, exhibit the inconsistency of the two schemes. This disagreement can be attributed to the fact that the Sigma-A method is more sensitive to local topographical features which highly affect the standard deviation of wind direction. This fact has serious implications in terms of concentration predictions using Gaussian models.

In order to examine the effect of the topography, land use and local flows on the turbulent state of the atmosphere in the region under study, the hourly evolution of Atmospheric Stability is studied for each station (see Figure 3).

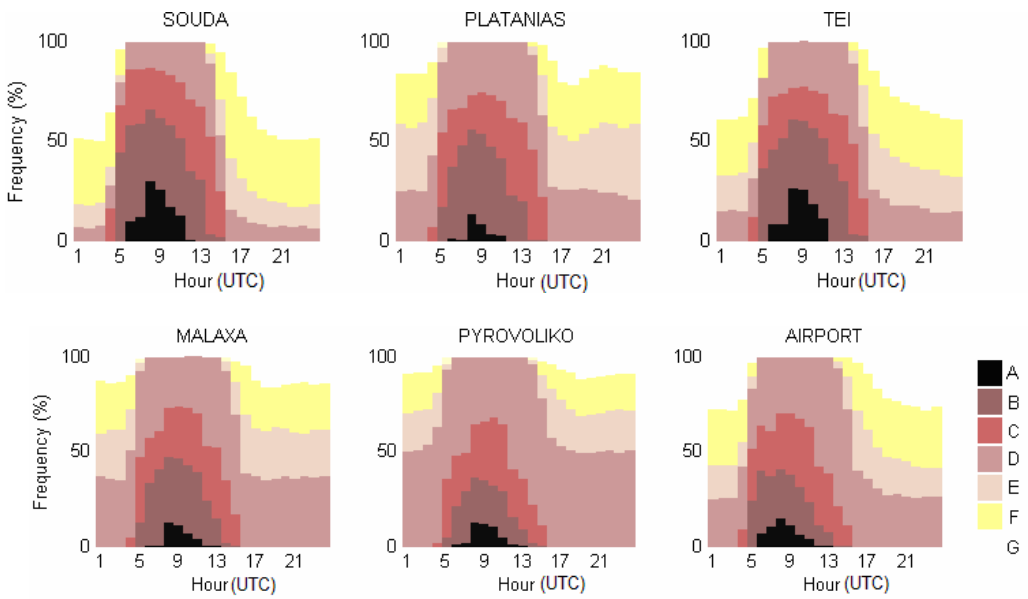

Figure 3: Hourly Frequency Distribution of Atmospheric Stability classes for each station.

The analysis shows that all stations follow a general daily pattern, where stable conditions prevail during the night and unstable during the daytime. Higher occurrences of extremely stable and highly unstable conditions are observed at the urban station of

TEI and the suburban station of Souda. Furthermore, the unstable conditions for these two stations persist until later in the afternoon compared to the other stations.

In order to assess the spatial homogeneity of Atmospheric Stability in the region under study, tables of joint frequencies for all possible pairs of stations are calculated. For this analysis we used the Turner scheme for calculating stability classes. In Table 2 we present the findings for Souda station.

Table 2: Joint–frequencies of occurrence (%) of stability classes compared to Souda station.

		PLATANIAS							MALAXA						
		A	B	C	D	E	F	G	A	B	C	D	E	F	G
SOUDA	A	**23.2**	69.8	6.9	0.1	--	--	--	**27.3**	59.9	12.5	0.3	--	--	--
	B	1.7	**59.8**	34.4	4.2	--	--	--	1.2	**48.3**	40.5	9.9	--	--	--
	C	0.0	7.1	**52.2**	40.6	--	--	--	0.0	3.5	**42.6**	53.9	--	--	--
	D	--	0.0	6.1	**89.6**	4.0	0.4	--	--	--	1.8	**97.4**	0.5	0.2	--
	E	--	--	--	50.3	**39.6**	9.5	0.5	--	--	--	83.8	**12.3**	3.5	0.4
	F	--	--	--	30.0	42.6	**23.9**	3.4	--	--	--	44.9	36.0	**17.4**	1.7
	G	--	--	--	1.6	24.5	41.7	**32.2**	--	--	--	6.8	26.4	40.2	**26.6**
		TEI							AIRPORT						
		A	B	C	D	E	F	G	A	B	C	D	E	F	G
SOUDA	A	**60.0**	38.4	1.6	--	--	--	--	**27.9**	46.8	25.3	--	--	--	--
	B	10.8	**71.6**	16.8	0.8	--	--	--	6.3	**38.5**	42.7	12.6			--
	C	0.2	14.4	**57.2**	28.2	--	--	--	0.3	2.6	**40.4**	56.6	--	--	--
	D	--	0.1	7.6	**88.2**	3.7	0.5	--	--	--	1.3	**97.9**	0.6	0.1	--
	E	--	--	--	37.4	**47.7**	12.7	2.1	--	--	--	78.5	**17.4**	4.0	0.1
	F	--	--	--	13.6	34.8	**42.9**	8.7	--	--	--	28.4	36.5	**34.3**	0.8
	G	--	--	--	0.4	3.0	26.7	**69.9**	--	--	--	1.2	10.1	38.7	**50.1**

		PYROVOLIKO							
		A	B	C	D	E	F	G	UNDEF.
SOUDA	A	**22.8**	34.9	27.5	1.7	--	--	--	13.1
	B	3.8	**26.4**	37.2	20.9			--	11.6
	C	0.2	2.7	**24.6**	58.5	--	--	--	13.9
	D	--	--	1.7	**80.5**	0.1	0.1	--	17.5
	E	--	--	--	73.5	**5.4**	1.6	0.1	19.4
	F	--	--	--	55.7	16.6	**10.7**	0.7	16.3
	G	--	--	--	19.9	26.2	25.7	**15.9**	12.2

All stations show a wide variation of stabilities, spreading over 4 categories lower or higher in comparison with Souda station. High agreement is observed only for neutral conditions (D). The TEI station exhibits the best agreement with percentages ranging from 60% for extremely unstable conditions (A) to 88.2% for neutral conditions (D).

2.3. Mixing Height Assessment

Atmospheric mixing height is the depth of the layer which is characterized by strong turbulent and convective mixing [5]. Owing to the lack of upper air measurements, the experimental Nozaki model [6] is adopted. It uses ground-level, routinely measured meteorological parameters. The mean hourly mixing height is estimated by the following formula [6]:

$$H = \frac{121 \cdot (6 - P) \cdot (T - T_d)}{6} + \frac{0.169 \cdot P \cdot (U + 0.257)}{12 \cdot f \cdot \ln(z / z_o)}$$

where H is the mean hourly mixing height in meters, P a meteorological parameter that depends on P-G stability class, T the ambient temperature, T_d the dew point temperature, U the wind speed at 10m, f the Coriolis parameter and z_o the surface roughness length.

In order to assess the spatial homogeneity of the mixing height, we employed the same methodology that used for the wind vector (similarity curves). Results of the Souda station are presented in Figure 4.

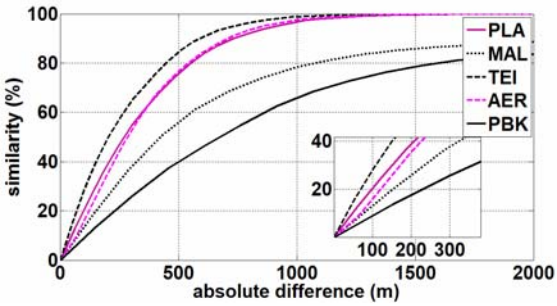

Figure 4: Similarity Degree of estimated Hourly Mixing Heights with respect to Souda station.

From Figure 4, it can be seen that the TEI station gives the most consistent estimations of mixing height in comparison to Souda. Furthermore, the similarity of the neighboring Souda and Malaxa stations is less than that of Souda and Platania or Airport. Thus confirming the highly in-homogeneity character of the area attributed to the intense topography which prevails in the South.

3. METEOROLOGICAL REPRESENTATIVENESS ASSESSMENT

Representativeness, is defined as 'the extent to which a set of measurements taken in a given space-time domain, reflect the actual conditions in the same or different space-time domain taken on a scale appropriate for a specific application" [7]. The greater area of the Chania Plain exhibits poor meteorological homogeneity and thus, a single representative station for the whole region cannot be selected. The spatial proximity of the available stations to the power plant is assessed by using Thiessen polygons, which represent the region of influence around each monitoring station. As can been seen in Figure 5, the Souda station is representative of the surrounding area of the power plant due to its proximity and resemblance in elevation, land-usage and cover.

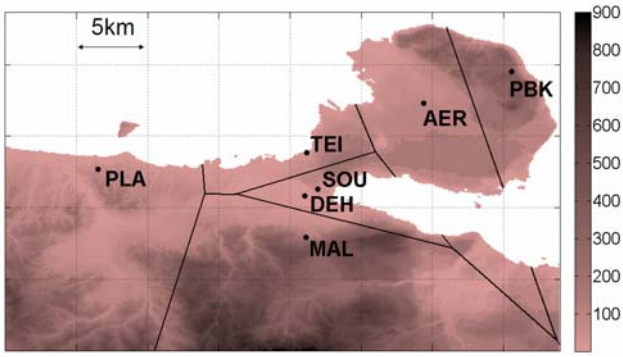

Figure 5: Spatial proximity polygons of the meteorological stations.

Whereas, the proximity of the meteorological monitoring site is an important factor, representativeness is not simply a function of distance. Wind direction and speed influence the horizontal representativeness by enlarging it towards the predominant wind direction [8]. In our case, the area corresponding to the Souda station can be extended

southwesterly, following the prevalent wind direction. The proximity to the sea towards the west is expected to significantly alter the results and thus, our modeling domain extends 1km to the West, East and the North of the power plant and 2km to the South.

4. CASE STUDIES USING A GAUSSIAN DISPERSION MODEL

A Gaussian plume model assumes that if a pollutant is emitted from a point source, the resulting concentration in the atmosphere, when averaged over sufficient time, will approximate a Gaussian distribution in space [9]. This is a good approximation for sufficiently long time averages. We applied a model that assumes the ground level and the inversion layer as perfect reflectors for pollutants. The estimated concentrations result from the following formula [10], [11]:

$$C = \frac{Q \cdot e^{-\frac{y^2}{2\sigma_y}}}{2\pi\sigma_y\sigma_z u}\left[e^{-\frac{(z-H)^2}{2\sigma_z^2}} + e^{-\frac{(z+H)^2}{2\sigma_z^2}} + \sum_{m=1}^{3}\left(e^{-\frac{(z+H+2mL)^2}{2\sigma_z^2}} + e^{-\frac{(z+H-2mL)^2}{2\sigma_z^2}} + e^{-\frac{(z-H+2mL)^2}{2\sigma_z^2}} e^{-\frac{(z-H-2mL)^2}{2\sigma_z^2}}\right)\right]$$

where Q the source emission rate, σ_y and σ_z the horizontal and vertical diffusion coefficients, u the horizontal wind speed, H the effective stack height and L the height of the mixing layer. The effective stack height is the sum of the physical stack height and the plume rise. The latter is calculated using Briggs Plume Rise equations [12], [13], [14].

We applied the model to estimate daily averages of sulphur dioxide ground-level concentrations, under various anemological conditions. The model is accurate in predicting the patterns of ground level concentrations. Higher concentrations result for the first two cases that correspond to low and medium wind speeds. As it is expected, in the third and fourth case, due to higher wind speeds, the transport mechanism leads to lower concentrations. The results of the model are in agreement with a previous study conducted in the area [15].

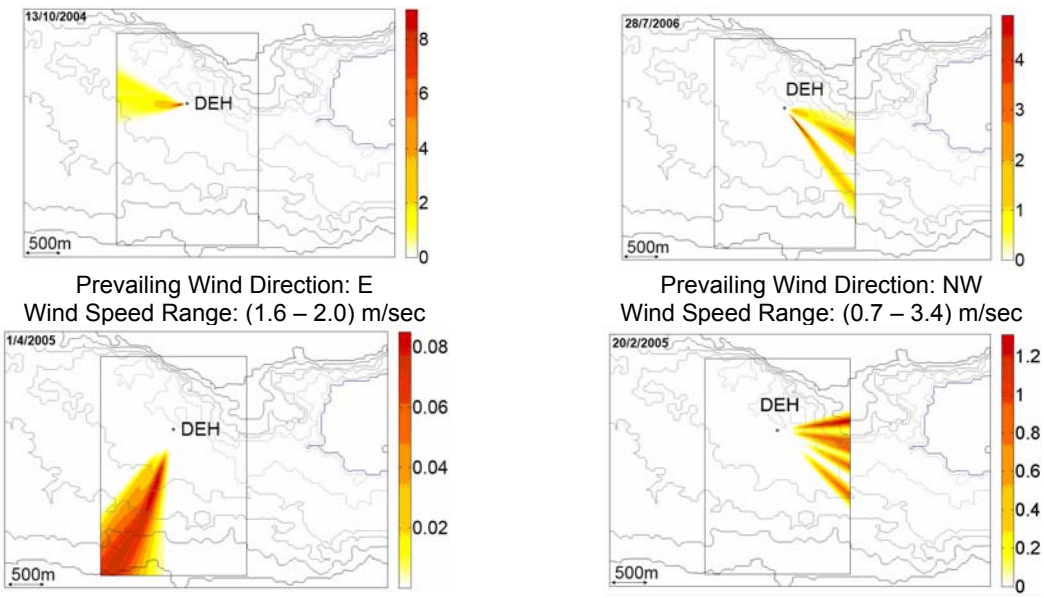

Prevailing Wind Direction: E
Wind Speed Range: (1.6 – 2.0) m/sec

Prevailing Wind Direction: NW
Wind Speed Range: (0.7 – 3.4) m/sec

Prevailing Wind Direction : NNE
Wind Speed Range: (1.7 – 5.6) m/sec

Prevailing Wind Direction : WNW
Wind Speed Range: (1.1 – 4.3) m/sec

Figure 6: Ground level estimated concentrations of SO_2 (μgr/m^3).

5. CONCLUSIONS

The results of this study prove that the greater area of the Chania Plain is non-homogeneous in terms of wind speed, wind direction, atmospheric stability and mixing height. This fact limits the spatial applicability of steady-state Gaussian models and therefore a sub-area of confidence needs to be defined. Taking into account the proximity and the similarities in land-usage and land-cover characteristics between the power plant and Souda station, an initial estimation of this sub-area is made. This area is further extended towards the South due to the impact of wind in spatial representivity. The numerical experiments of the case studies indicate that such a model is capable of predicting the general pattern of ground-level concentrations of SO_2 in the proximate area of the power plant.

ACKNOWLEDGEMENTS

The work described in this paper has been funded by the European Social Fund and Hellenic National Resources under the PYTHAGORAS II programme (EPEAEK II).

REFERENCES

1. Hazelton M.L. and Turlach B.A. (2007) 'Reweighted Kernel Density Estimation', *Computational Statistics & Data Analysis*, **51(6)**, 3057-3069.
2. Pasquill F. (1961) 'The estimation of the dispersion of windborne material', *Meteorol. Mag.*, **90**, 33-49.
3. Turner D.B. (1964) 'A diffusion model for an urban area', *J. Appl. Meteor.*, **3**, 83-91.
4. Bailey D.T. (2000) 'Meteorological Monitoring Guidance for Regulatory Modeling Applications', *Report, U.S. Environmental Protection Agency*.
5. Ulke A.G. and Mazzeo N.A. (1998) 'Climatological aspects of the daytime mixing height in Buenos Aires City, Argentina', *Atmospheric Environment*, **32(9)**, 1615-1622.
6. Cheng S.Y., Huang G.H., Chakma A., Hao R.X., Liu L. and Zhang X.H. (2001) 'Estimation of Atmospheric Stability Mixing Heights using data from Airport Meteorological Stations', *J. Environ. Sci. Health,* **A36(4)**, 521 – 532.
7. Nappo C.J., Caneill J.Y., Furman R.W., Gifford F.A., Kaimal J.C., Kramer M.L., Lockhart T.J., Pendergast M.M, Pielke R.A., Randerson D., Shreffler J.H. and Wyngaard J.C. (1982) 'The Workshop on the Representativeness of Meteorological Observations', *Bull. Am. Meteorol. Soc.*, **63**, 761-764.
8. Knoderer C. (2004) 'CRPAQS Surface and Aloft Meteorological Representativeness', URL: http://www.sonomatechdata.com/crpaqsmetrep/index.cfm
9. Shieh L.J., Halpern P.K., Clemens B.A., Wang H.H. and Abraham F.F. (1972) 'Air Quality Diffusion Model; Application to New York City', *IMB Journal Research Development.*
10. Beychok M. R. (2005) 'Fundamentals Of Stack Gas Dispersion', 4th Edition, author-published.
11. Essa K.S.M., Etman S.M. and Embaby M.(2003) 'Air pollutant concentration and its location under different thermal stability classes', *Meteorology and Atmospheric Physics,* **83**, 123-129.
12. Hanna S.R., Briggs G.A. and Hosker R.P. Jr. (1982) 'Handbook on Atmospheric Diffusion', *Technical Information Center U.S. Department of Energy.*
13. Briggs G.A. (1971) 'Some recent analyses of plume rise observation', *Second International Clean Air Congress Proceedings*, Academic Press, New York.
14. Briggs, G.A. (1972) 'Discussion: chimney plumes in neutral and stable surroundings', *Atmos. Envir.*, **6**, 507-510.
15. Deligiorgi D. (2006) 'Study of Atmospheric Dispersion in complex topography in conjunction with Atmospheric Stability – Numerical Model Application', *Technical Report*, Department of Physics, National and Kapodistrian University of Athens.